Structural Engineering and Mechanics, Vol. 26, No. 5 (2007) 591-615
DOI: http://dx.doi.org/10.12989/sem.2007.26.5.591

A BEM implementation for 2D problems in plane orthotropic elasticity

N. Kadioglu† and S. Ataoglu‡

Division of Mechanics, Civil Engineering Department, Faculty of Civil Engineering, Istanbul Technical University, Maslak 34469 Istanbul, Turkey

(Received March 27, 2006, Accepted February 5, 2007)

Abstract. An improvement is introduced to solve the plane problems of linear elasticity by reciprocal theorem for orthotropic materials. This method gives an integral equation with complex kernels which will be solved numerically. An artificial boundary is defined to eliminate the singularities and also an algorithm is introduced to calculate multi-valued complex functions which belonged to the kernels of the integral equation. The chosen sample problem is a plate, having a circular or elliptical hole, stretched by the forces parallel to one of the principal directions of the material. Results are compatible with the solutions given by Lekhnitskii for an infinite plane. Five different orthotropic materials are considered. Stress distributions have been calculated inside and on the boundary. There is no boundary layer effect. For comparison, some sample problems are also solved by finite element method and to check the accuracy of the presented method, two sample problems are also solved for infinite plate.

Keywords: elasticity; orthotropy; finite plates having elliptical and circular holes; multi-valued function; boundary element; reciprocity theorem; singularity.

1. Introduction

Stress and displacement analyses in anisotropic elasticity are of interest in mechanics of composites or geomechanics. Analytical solutions of some basic problems of this subject were investigated by Lekhnitskii (1947, 1963, 1968). The use of reciprocity theorem or Somigliana's integral identity is an effective method for the solutions of anisotropic elasticity problems. This method gives an integral equation. In the absence of the body forces this equation involves only surface integrals. Boundary Element Method deals with the numerical solution of this integral equation.

Rizzo and Shippy (1970) derived a real variable integral formula. Benjumea and Sikarskie (1972) applied the integral equation techniques to problems of plane orthotropic elasticity. Heng (1988) presented a technique to modify the boundary element method and solved some elastostatic problems by using constant elements. Vable and Sikarskie (1988) solved the orthotropic plate with circular hole for a few different materials using linear elements. Deb and Banerjee (1990) considered body forces. Jiang and Lee (1994) developed a numerical approach for the stress

† Associate Professor, E-mail: kadiog@itu.edu.tr
‡ Associate Professor, E-mail: ataoglu@itu.edu.tr

analysis of anisotropic layers under various loading conditions. Mantič and París (1995) presented a complex formulation of the fundamental displacements and tractions following Lekhnitskii and Stroh theories. Raju *et al.* (1996) presented a method for two-dimensional orthotropic problems. Padhi *et al.* (2000) investigated the real variable fundamental solution approach to the Boundary Integral Equation method in two-dimensional orthotropic elasticity, using quadratic isoparametric elements. Tsutsumi and Hirashima (2000) presented the circular disks or rings under diametrical loadings. Berbinau and Soutis (2001) worked to solve mixed boundary value problems along holes in composite plates. Lee *et al.* (2001) presented an analysis for the displacement and stress fields of an unbounded isotropic matrix, containing orthotropic cylindrical inclusions and voids. Avila *et al.* (1997) investigated the stress distribution in and on the boundary.

Some singularity problems arise in the solution of integral equation mentioned above. Besides, there are some difficulties in the calculation of the unknown stress component on the boundary. This problem is named as boundary layer effect. In this study, whole singularities are eliminated and the unknown stress component are calculated on the boundary. In the previous study of Kadioglu and Ataoglu (1999), these two problems had been solved for isotropic materials. Here, in addition, a new algorithm is also introduced to calculate multi-valued complex functions. The fundamental solution, which given by Mantič and París (1995), is used in this study.

Some specific problems are solved to check accuracy of the formulation, for different orthotropic materials. The present results are seen to be better than those obtained by others, and, they are compatible with Lekhnitskii's (1947, 1963, 1968).

2. Basic formulation

The definition of a plane problem of orthotropic elasticity is summarized below.

A region B with interior volume V and boundary S is considered. The material filling V is orthotropic. The ordered pair $S(\mathbf{u}(\mathbf{x}), \mathbf{T}(\mathbf{x}))$ define a problem in region B. $\mathbf{u}(\mathbf{x}), \mathbf{T}(\mathbf{x})$ denote the displacement vector and the stress tensor respectively. $\mathbf{x}$ is the position vector of an arbitrary point. For an orthotropic material, they satisfy following relations.

$$T_{kj,j} + f_k = 0 \tag{1}$$

$$\varepsilon_{kj} = \frac{1}{2}\left(\frac{\partial u_k}{\partial x_j} + \frac{\partial u_j}{\partial x_k}\right) \quad (k, j = 1, 2) \tag{2}$$

$$\begin{aligned} \varepsilon_{11} &= \beta_{11}T_{11} + \beta_{12}T_{22} \\ \varepsilon_{22} &= \beta_{12}T_{11} + \beta_{22}T_{22} \\ \varepsilon_{12} &= 0.5\beta_{66}T_{12} \end{aligned} \tag{3}$$

where $\boldsymbol{\varepsilon}$ is the strain tensor, β_{kj} represents the elastic constants of the material. $\mathbf{f}$ denotes the body force. The expression of reciprocal identity which is written between two different problems, $S(\mathbf{u}, \mathbf{T})$ and $S^*(\mathbf{u}^*, \mathbf{T}^*)$, for the same body is

$$\int_S \mathbf{t}^* \cdot \mathbf{u}dS + \int_V \mathbf{f}^* \cdot \mathbf{u}dV = \int_S \mathbf{t} \cdot \mathbf{u}^* dS + \int_V \mathbf{f} \cdot \mathbf{u}^* dV \tag{4}$$

$$t_k = T_{kj}n_j,\ t_k^* = T_{kj}^* n_j \tag{5}$$

$\mathbf{t}$ and $\mathbf{t}^*$ are surface traction vectors in two problems respectively, $\mathbf{n}$ is the outward normal of the surface S. It will be considered that $S(\mathbf{u}, \mathbf{T})$ represents a problem to be solved on the region B of volume V bounded by surface S. In plane problems, V is reduced to a simple or multiply connected planar region. From now on $S(\mathbf{u}, \mathbf{T})$ is considered as the first boundary value problem, (Sokolnikoff 1956). But the solution method can be applied to the second boundary value and mixed boundary value problems as well. The second problem $S^*(\mathbf{u}^*, \mathbf{T}^*)$ is named as a fundamental or singular solution and it represents the displacement and stress fields in an unbounded plane medium due to a point load applied at a specific point $\mathbf{y}$.

3. Fundamental solution

A body force in an orthotropic, infinite planar medium having the same elastic constants with the problem to be solved is defined as

$$\mathbf{f}^k = \delta(\mathbf{x}-\mathbf{y})\mathbf{e}_k \tag{6}$$

where $\mathbf{x}$ and $\mathbf{y}$ represent the position vectors of an arbitrary point and a specific point of the medium respectively. $\mathbf{e}_k(k = 1, 2)$ indicates a base vector in Cartesian coordinates. $\delta(\mathbf{x}-\mathbf{y})$ is a generalized function, which is known as Dirac delta function satisfying the following property

$$\begin{aligned} \int_V \mathbf{h}(\mathbf{x})\delta(\mathbf{x}-\mathbf{y})dV_x &= \mathbf{h}(\mathbf{y}) \quad \text{for} \quad \mathbf{y} \in V \\ &= \mathbf{0} \qquad \text{for} \quad \mathbf{y} \notin V \end{aligned} \tag{7}$$

The solution of this problem can be represented as $S^k(\mathbf{u}^k, \mathbf{T}^k)$. This solution is given by Mantič and París (1995) for different types of orthotropic materials as below.

$$u_l^k(\mathbf{x}, \mathbf{y}) = \mathbf{Re}\left\{\left(\frac{1}{i\pi}\right)\sum_{\lambda=1}^{2} P_{l\lambda}P_{k\lambda}(1/\kappa_\lambda^2)\mathbf{ln}z_\lambda\right\} \tag{8}$$

$$t_l^k(\mathbf{x}, \mathbf{y}) = -\mathbf{Re}\left\{\left(\frac{1}{i\pi}\right)\sum_{\lambda=1}^{2} \frac{1}{\kappa_\lambda^2}P_{k\lambda}Q_{l\lambda}(1/z_\lambda)(\mu_\lambda n_1 - n_2)\right\} \tag{9}$$

$$i = \sqrt{-1}$$

The quantities in these two expressions are defined depending on two complex constants $\mu_\lambda(\lambda = 1, 2)$, defined in terms of β_{ij} coefficients, as the two of the roots of the following nonlinear equation, (Lekhnitskii 1963, Mantič and París 1995).

$$\beta_{11}\mu^4 + (2\beta_{12} + \beta_{66})\mu^2 + \beta_{22} = 0 \tag{10}$$

There are two cases for μ_λ values $\lambda = 1, 2$

for $(2\beta_{12} + \beta_{66}) > 2\sqrt{\beta_{11}\beta_{22}}$

$$\mu_1 = \frac{i}{\sqrt{2\beta_{11}}}\sqrt{2\beta_{12} + \beta_{66} + \sqrt{(2\beta_{12} + \beta_{66})^2 - 4\beta_{11}\beta_{22}}}$$

$$\mu_2 = \frac{i}{\sqrt{2\beta_{11}}}\sqrt{2\beta_{12} + \beta_{66} - \sqrt{(2\beta_{12} + \beta_{66})^2 - 4\beta_{11}\beta_{22}}} \tag{11}$$

for $(2\beta_{12} + \beta_{66}) < 2\sqrt{\beta_{11}\beta_{22}}$

$$\mu_1 = c + id, \quad \mu_2 = -c + id$$

where

$$c = \frac{i}{\sqrt{2\beta_{11}}}\sqrt{\sqrt{\beta_{11}\beta_{22}} - \left(\beta_{12} + \frac{\beta_{66}}{2}\right)}$$

$$d = \frac{i}{\sqrt{2\beta_{11}}}\sqrt{\sqrt{\beta_{11}\beta_{22}} + \left(\beta_{12} + \frac{\beta_{66}}{2}\right)} \tag{12}$$

In terms of μ_λ values, **Q**, **P** and **κ** constant matrices are defined as follows

$$\mathbf{Q} = \begin{bmatrix} -\mu_1 & -\mu_2 \\ 1 & 1 \end{bmatrix}, \quad \mathbf{P} = \begin{bmatrix} \beta_{11}\mu_1^2 + \beta_{12} & \beta_{11}\mu_2^2 + \beta_{12} \\ \beta_{12}\mu_1 + \dfrac{\beta_{22}}{\mu_1} & \beta_{12}\mu_2 + \dfrac{\beta_{22}}{\mu_2} \end{bmatrix} \tag{13}$$

$$\boldsymbol{\kappa} = \mathbf{P}^T\mathbf{Q} + \mathbf{Q}^T\mathbf{P} = \begin{bmatrix} \kappa_1^2 & 0 \\ 0 & \kappa_2^2 \end{bmatrix} = 4i\sqrt{\beta_{11}\beta_{22} - \left(\beta_{12} + \frac{\beta_{66}}{2}\right)^2}\begin{bmatrix} -\mu_1 & 0 \\ 1 & \mu_2 \end{bmatrix} \tag{14}$$

There are only two $z_\lambda(\lambda = 1, 2)$ variables in Eqs. (8) and (9) defined as

$$z_\lambda = (x_1 - y_1) + \mu_\lambda(x_2 - y_2) \tag{15}$$

For a first boundary value problem, $S(\mathbf{u}, \mathbf{T})$, in orthotropic plane elasticity the expression of the reciprocal identity (Eq. (4)) which is written between $S(\mathbf{u}, \mathbf{T})$ and $S^* = S^k(\mathbf{u}^k, \mathbf{T}^k)$, neglecting body forces, is reduced to the following form

$$\begin{aligned} \int_S \mathbf{t}(\mathbf{x}) \cdot \mathbf{u}^k(\mathbf{x}, \mathbf{y})dS_x - \int_S \mathbf{u}(\mathbf{x}) \cdot \mathbf{t}^k(\mathbf{x}, \mathbf{y})dS_x &= u_k(\mathbf{y}) \quad \text{for} \quad \mathbf{y} \in V, \mathbf{y} \notin S \\ &= 0 \quad \text{for} \quad \mathbf{y} \notin V, \mathbf{y} \notin S \end{aligned} \tag{16}$$

Using Eq. (16) and Eq. (2) the components of the strain tensor become

$$\begin{aligned} \varepsilon_{lj}(\mathbf{y}) &= 0.5\int_S \mathbf{t}(\mathbf{x}) \cdot (\mathbf{u}^{lj}(\mathbf{x}, \mathbf{y}) + \mathbf{u}^{jl}(\mathbf{x}, \mathbf{y}))dS_x \\ &- 0.5\int_S \mathbf{u}(\mathbf{x}) \cdot (\mathbf{t}^{lj}(\mathbf{x}, \mathbf{y}) + \mathbf{t}^{jl}(\mathbf{x}, \mathbf{y}))dS_x \quad \text{for} \quad \mathbf{y} \in V, \ \mathbf{y} \in S \end{aligned} \tag{17}$$

where

$$u_l^{kj}(\mathbf{x},\mathbf{y}) = \frac{\partial u_l^k(\mathbf{x},\mathbf{y})}{\partial y_j} = -\mathbf{Re}\left\{\left(\frac{1}{i\pi}\right)\sum_{\lambda=1}^{2} P_{k\lambda}P_{l\lambda}(1/\kappa_\lambda^2)(1/z_\lambda)\frac{\partial z_\lambda}{\partial x_j}\right\} \tag{18}$$

$$t_l^{kj}(\mathbf{x},\mathbf{y}) = \frac{\partial t_l^k(\mathbf{x},\mathbf{y})}{\partial y_j} = \mathbf{Re}\left\{\left(\frac{1}{i\pi}\right)\sum_{\lambda=1}^{2} P_{k\lambda}Q_{l\lambda}(1/\kappa_\lambda^2)(1/z_\lambda^2)\frac{\partial z_\lambda}{\partial x_j}(\mu_\lambda n_1 - n_2)\right\} \tag{19}$$

For the first fundamental problem, (Sokolnikoff 1956), the surface traction vector $\mathbf{t}(\mathbf{x})$ is given on the boundary S of the region V. The expressions (8), (9) and (11) to (15) can be found in the study of Mantič and París (1995). But the right-side of Eq. (16) has been given as $C_{kl}u_l(\mathbf{y})$ for $\mathbf{y} \in S, \mathbf{y} \notin V$ in their study. This term is named as free term in literature and C_{kl} is kl component of $\mathbf{C}$ matrix.

The details have been given in Mantič and París (1995). But their formulation involving $\mathbf{C}$ matrix has not been used in this study.

For a multiply connected region, the boundary S contains a finite number of disjoint curves and an integral over S is equal to the summation of the integrals over these disjoint curves. It is clear that, for the first fundamental problem, the displacement vector can be calculated from Eq. (16) at any arbitrary point $\mathbf{y}$ of the region if the displacement field is known on the boundary. Then using Eqs. (17) and (3), the stress components can be calculated at $\mathbf{y}$. In that case, the solution of the problem is reduced to calculate the displacement field $\mathbf{u}(\mathbf{x})$ on the boundary S by solving integral equation given in Eq. (16). The solution of this integral equation is explained below:

Boundary S is idealized as a collection of line segments. If the number of these line segments is N, the number of the end points, named as nodal points is also N for a closed boundary. It is assumed that the variation of any displacement component on a line segment is linear. Then the unknowns of the problem are reduced to the values of the displacement components at nodal points. $2N$ integral equations each one of them corresponding to a singular loading at a nodal point in one direction can be written. In these integral equations, integrals over the boundary are transformed to the summation of the integrals over the line segments. In addition, an artificial boundary including all of the line segments but not the nodal point $\mathbf{x}(I)$, will be defined for a singular loading on that nodal point (Fig. 1). Around $\mathbf{x}(I)$ a small circular arc, S_ε, which leaves the point outside the region is added to complete this artificial boundary.

It is assumed that the displacement components are constant and the components of surface traction vector are equal to zero on this circular arc S_ε. As a consequence of the definition of the

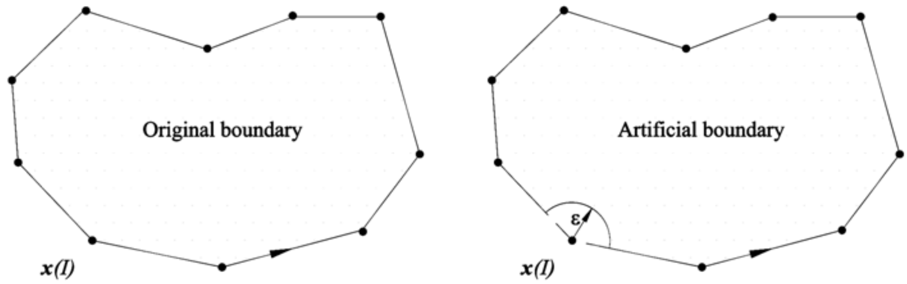

Fig. 1 Representation of the artificial boundary

artificial boundary if $\mathbf{y}$ is a nodal point $\mathbf{x}(I)$, right side of the Eq. (16) becomes zero because $\mathbf{y}$ is not a point in the region bounded by this artificial boundary. After necessary calculations the radius ε, of the circular arc will be shrunk to the nodal point $\mathbf{x}(I)$. The first assumption on circular arc, S_ε, means that any displacement component at a nodal point is single-valued. The second assumption is that there is not a singular force acting at that nodal point. The integrals of $t_l^k(\mathbf{x}, \mathbf{y})$ functions over the circular arc coincide with C_{kl} (Mantič and París 1995) for some special cases. After all these assumptions Eq. (16) is reduced to a system of linear algebraic equations as below

$$\mathbf{AU} = \mathbf{K} \tag{20}$$

where $\mathbf{A}$ is a $2N$ by $2N$ matrix, and whose components defined as

$$A_{IJ} = \delta_{IJ}\int_{S_\varepsilon} t_1^1(\mathbf{x}, \mathbf{x}(J))ds + \int_0^{l(J)}\left\{t_1^1(\mathbf{x}, \mathbf{x}(I))\left[1 - \frac{s}{l(J)}\right]\right\}ds + \int_0^{l(J-1)}\left\{t_1^1(\mathbf{x}, \mathbf{x}(I))\left[\frac{s}{l(J-1)}\right]\right\}ds$$

$$A_{I(J+N)} = \delta_{IJ}\int_{S_\varepsilon} t_2^1(\mathbf{x}, \mathbf{x}(J))ds + \int_0^{l(J)}\left\{t_2^1(\mathbf{x}, \mathbf{x}(I))\left[1 - \frac{s}{l(J)}\right]\right\}ds + \int_0^{l(J-1)}\left\{t_2^1(\mathbf{x}, \mathbf{x}(I))\left[\frac{s}{l(J-1)}\right]\right\}ds$$

$$A_{(I+N)J} = \delta_{IJ}\int_{S_\varepsilon} t_1^2(\mathbf{x}, \mathbf{x}(J))ds + \int_0^{l(J)}\left\{t_1^2(\mathbf{x}, \mathbf{x}(I))\left[1 - \frac{s}{l(J)}\right]\right\}ds + \int_0^{l(J-1)}\left\{t_1^2(\mathbf{x}, \mathbf{x}(I))\left[\frac{s}{l(J-1)}\right]\right\}ds$$

$$A_{(I+N)(J+N)} = \delta_{IJ}\int_{S_\varepsilon} t_2^2(\mathbf{x}, \mathbf{x}(J))ds + \int_0^{l(J)}\left\{t_2^2(\mathbf{x}, \mathbf{x}(I))\left[1 - \frac{s}{l(J)}\right]\right\}ds + \int_0^{l(J-1)}\left\{t_2^2(\mathbf{x}, \mathbf{x}(I))\left[\frac{s}{l(J-1)}\right]\right\}ds$$

$$\text{for} \quad I, J = 1, N \tag{21}$$

where δ_{IJ} represents Kronecker's delta and $l(J)$ is the length of the Jth linear segment. $\mathbf{U}$ and $\mathbf{K}$ are matrices of order $2N$ by 1 defined as

$$\begin{aligned} U_I &= u_1(\mathbf{x}(I)) \quad \text{for} \quad I = 1, N \\ U_{(I+N)} &= u_2(\mathbf{x}(I)) \quad \text{for} \quad I = 1, N \\ K_I &= \sum_{J=1}^{N}\int_0^{l(J)}[u_1^1(\mathbf{x}, \mathbf{x}(I))t_1(\mathbf{x}) + u_2^1(\mathbf{x}, \mathbf{x}(I))t_2(\mathbf{x})]ds \quad \text{for} \quad I = 1, N \\ K_{(I+N)} &= \sum_{J=1}^{N}\int_0^{l(J)}[u_1^2(\mathbf{x}, \mathbf{x}(I))t_1(\mathbf{x}) + u_2^2(\mathbf{x}, \mathbf{x}(I))t_2(\mathbf{x})]ds \quad \text{for} \quad I = 1, N \end{aligned} \tag{22}$$

Before limit process $(\varepsilon \to 0)$ the integrals over a circular arc S_ε, see Fig. 2, about a nodal point $\mathbf{x}(I)$ are reduced to the calculation of the integral given below.

$$I_\lambda = \int_{\theta_1}^{\theta_2}(\mu_\lambda n_1 - n_2)\frac{1}{z_\lambda}ds \tag{23}$$

Substituting $n_1 = -\cos\theta, n_2 = -\sin\theta, z_\lambda = \varepsilon\cos\theta + \varepsilon\mu_\lambda\sin\theta$ and $ds = -\varepsilon d\theta$

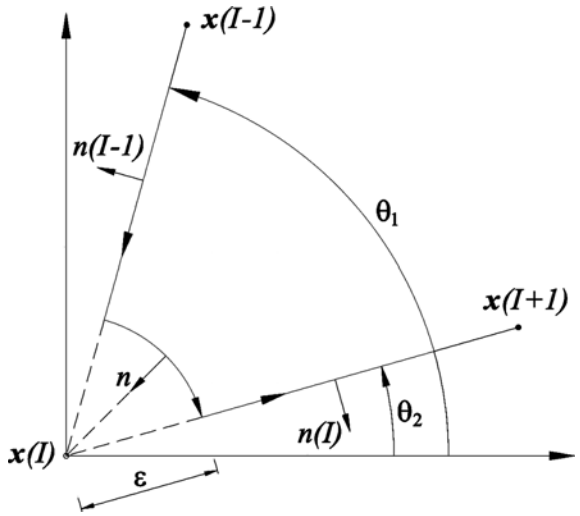

Fig. 2 Representation of the circular arc S_ε

$$I_\lambda = \ln\sqrt{\cos^2\theta + \mu_\lambda^2\sin^2\theta + 2\mu_\lambda\cos\theta\sin\theta} + i\arctan\left(\frac{\mathrm{Im}(\mu_\lambda\sin\theta)}{\cos\theta + \mathrm{Re}(\mu_\lambda\sin\theta)}\right)\Big|_{\theta_1}^{\theta_2} \tag{24}$$

is obtained. In order to calculate the imaginary part of this integral, the following algorithm is developed

for	$\theta_2 - \pi \le \theta_1$	$\phi_2 = \theta_2$
for	$\theta_2 - \pi > \theta_1$	$\phi_2 = -(2\pi - \theta_2)$
for	$\theta_1 - \pi < \theta_2$	$\phi_1 = \theta_1$
for	$\theta_1 - \pi \ge \theta_2$	$\phi_1 = -(2\pi - \theta_1)$

$$\beta_1 = \arctan\frac{\mathrm{Im}(\mu_\lambda)\sin\phi_1}{\cos\phi_1 + \mathrm{Re}(\mu_\lambda)\sin\phi_1}$$

$$\beta_2 = \arctan\frac{\mathrm{Im}(\mu_\lambda)\sin\phi_2}{\cos\phi_2 + \mathrm{Re}(\mu_\lambda)\sin\phi_2}$$

for	$(\beta_2 - \beta_1) < 0$	$\mathrm{Im}(I_\lambda) = \beta_2 - \beta_1$
for	$(\beta_2 - \beta_1) \ge 0$	$\mathrm{Im}(I_\lambda) = \beta_2 - \beta_1 - 2\pi$

Other integrals over line segments, see Fig. 3, in Eqs. (21) can be reduced to the combination of the following two integrals

$$R_\lambda = \int_0^{l(J)} \frac{1}{z_\lambda}(\mu_\lambda n_1 - n_2)ds = \left|\ln(z_\lambda)\right|_{s=0}^{l(J)}$$

$$Q_\lambda = \int_0^{l(J)} \frac{1}{z_\lambda}(\mu_\lambda n_1 - n_2)\frac{s}{l(J)}ds = \left|\ln(z_\lambda)\frac{s}{l(J)} - \frac{1}{l(J)(\mu_\lambda n_1 - n_2)}z_\lambda(\ln(z_\lambda) - 1)\right|_{s=0}^{l(J)} \tag{25}$$

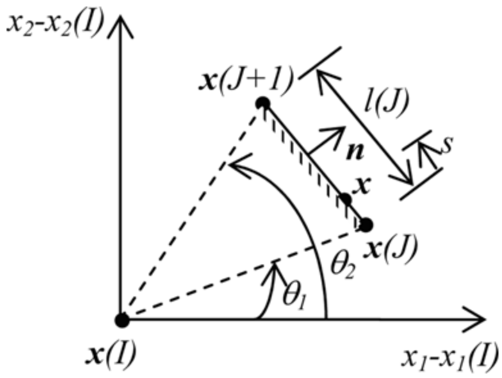

Fig. 3 The boundary element of the number J

where

$$\begin{aligned} z_\lambda &= -n_2 s + x_1(J) - x_1(I) + \mu_\lambda (n_1 s + x_2(J) - x_2(I)) \\ dz_\lambda &= (\mu_\lambda n_1 - n_2) ds \end{aligned} \tag{26}$$

It is seen from Eqs. (25) that another difficulty arises in the calculation of the end values of multi-valued function $\ln(z_\lambda)$. To calculate their imaginary parts, an archive function program has been written to calculate all of the values of the arctan function on the interval $[0, 2\pi]$. This makes possible to achieve a single value for arctan function in this interval.

Then, the following algorithm is introduced

$$\mathrm{Im}(\ln(z_\lambda)) = \phi_2 - \phi_1 \tag{27}$$

where

$$\beta_1 = \arctan\left(\frac{\sin\theta_1 \mathrm{Im}\mu_\lambda}{\cos\theta_1 + \sin\theta_1 \mathrm{Re}\mu_\lambda}\right), \quad \beta_2 = \arctan\left(\frac{\sin\theta_2 \mathrm{Im}\mu_\lambda}{\cos\theta_2 + \sin\theta_2 \mathrm{Re}\mu_\lambda}\right)$$

$$\begin{array}{lll}
\text{For } \beta_1 > \beta_2 & & \phi_2 = \beta_2 \\
\quad \text{for } \beta_1 \geq \beta_2 + \pi & \Rightarrow & \phi_1 = -(2\pi - \beta_1) \\
\quad \text{for } \beta_1 < \beta_2 + \pi & \Rightarrow & \phi_1 = \beta_1 \\
\text{for } \beta_1 = \beta_2 & \Rightarrow & \phi_2 = \beta_2 \\
 & & \phi_1 = \beta_1 \\
\text{for } \beta_1 < \beta_2 & & \phi_1 = \beta_1 \\
\quad \text{for } \beta_2 \leq \beta_1 + \pi & \Rightarrow & \phi_2 = \beta_2 \\
\quad \text{for } \beta_2 > \beta_1 + \pi & \Rightarrow & \phi_2 = -(2\pi - \beta_2)
\end{array}$$

Since z_λ is a single-valued function using the same way the imaginary part of Q_λ can also be calculated. A third difficulty arises in the calculation of the real part of R_λ. This term involves a singularity on each of the two line segments joining at a nodal point on which a singular loading exists in any direction. But the coefficient of any displacement component at this nodal point, in the linear algebraic equation which corresponds to the loading at the same point, does not involve any singularity because the singular terms arising in adjacent elements eliminate each other.

Following this algorithm all integrals over the line segments can be calculated analytically.

After determination of the matrices, **A** and **K**, the unknown matrix **U** is calculated by solving Eq. (20). For calculation of any strain component at any **y** point, to use the calculated nodal values of the displacement components in Eq. (17) is enough. New integrals, arising in this process, can be reduced to the same integrals mentioned above by partial integration. There are some other integrals, but they are single-valued.

If the loading point **y** is on the boundary, this corresponds to the case of $\theta_1 = \theta_2 \pm \pi$ which considered before, see Fig. 3, during calculation of $\mathrm{Im}(R_\lambda)$. Here, there is only one restriction that it is not possible to calculate the stress components at the nodal points. If it is needed to calculate the stress components at a point, this point must not be selected as a nodal point. And if there is a singular force applied at a point on the boundary, this point cannot be selected as a nodal point either because of our second assumption on circular arc, S_ε.

4. Examples

Two types of sample problems were selected to compare the present method with the other theoretical (Lekhnitskii 1947, 1963, 1968) and numerical studies (Vable and Sikarskie 1988) and (Raju *et al.* 1996).

The first problem is a square orthotropic plate having a circular hole stretched by tensile stresses parallel to x_1 axis (Fig. 4(a)).

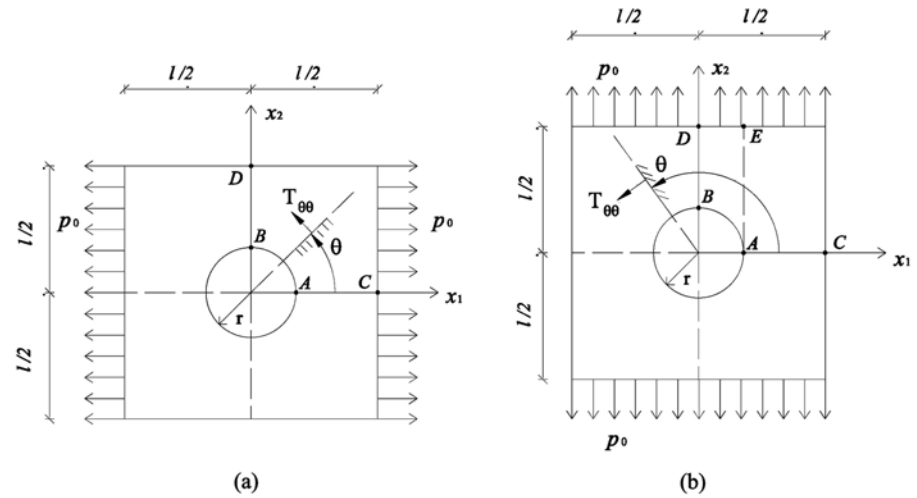

Fig. 4 Sample problem 1(a) and 1(b)

Table 1 Material constants (1/MPa)

	Material I	Material II	Material III
β_{11}	1/12000	1/6000	1/200000
β_{22}	1/6000	1/12000	1/200000
β_{12}	−0.071/12000	−0.036/6000	−0.25/200000
β_{66}	1/700	1/700	1.65/200000

Three different materials are considered. Material constants are given in Table 1.

Material I and II are selected to be the same as those used in Lekhnitskii's (1963) theoretical solution for an infinite plate and Material I is also used by Raju *et al.* (1996). Both μ_1 and μ_2 are pure imaginary for the cases of material I and II. Material III is selected to consider the case given by Eqs. (12). The region of the problem is multiply connected. $4N$ nodal points are selected on the boundary and the whole boundary is considered. It seems that the number of the nodal points is more than that employed in each of the other studies, but by taking advantage of the existing quarter symmetry the number of equations to be solved is reduced from $8N$ to $2N$ (Fig. 5).

It must be emphasized that there is not any nodal point inside the region. For this problem, it is important to calculate the values of the stress component $T_{\theta\theta}$ at the boundary points A and B of the cavity (Fig. 4), which lie on the symmetry axes, so these points were not selected as nodal points.

In this study, 32 and 128 are the maximum numbers of the used nodal points on the external and internal boundaries, respectively. Because of the quarter symmetry, the maximum number of the

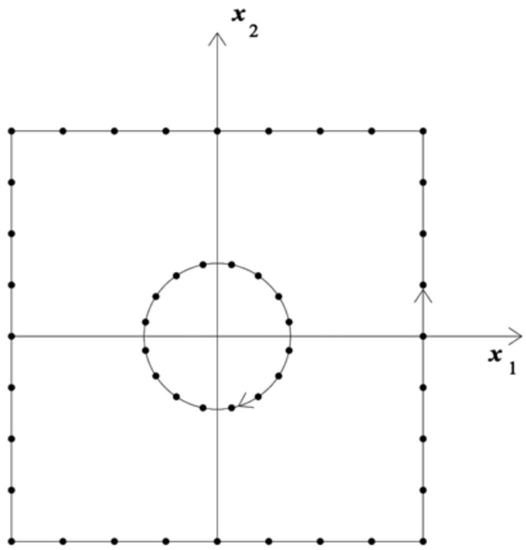

Fig. 5 Nodal points

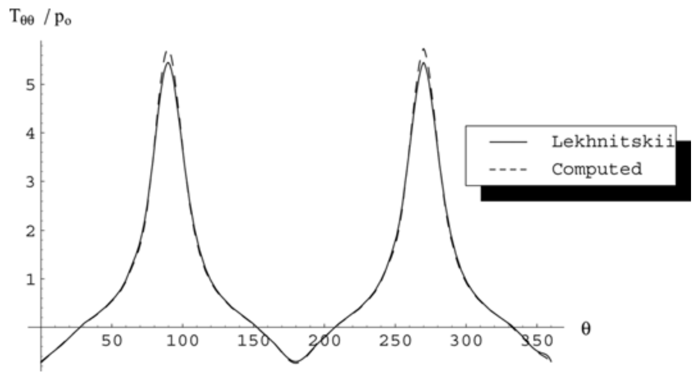

Fig. 6 Variation of dimensionless stress component, $T_{\theta\theta}/p_o$, versus θ, on the circular cavity for material I and problem 1(a), $l = 100$ cm, $r = 0.5$ cm

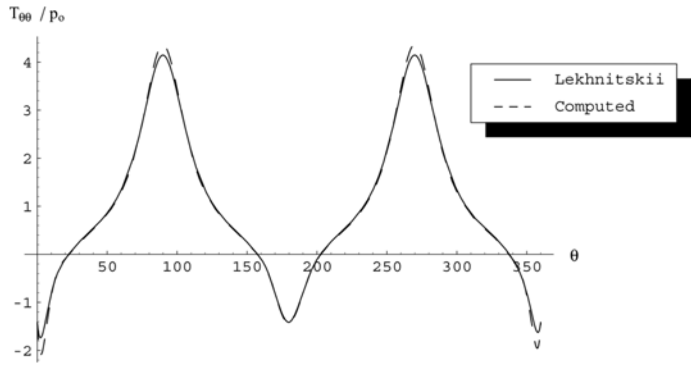

Fig. 7 Variation of dimensionless stress component, $T_{\theta\theta}/p_o$, versus θ on the circular cavity for material II and problem 1(a), $l = 100$ cm, $r = 0.5$ cm

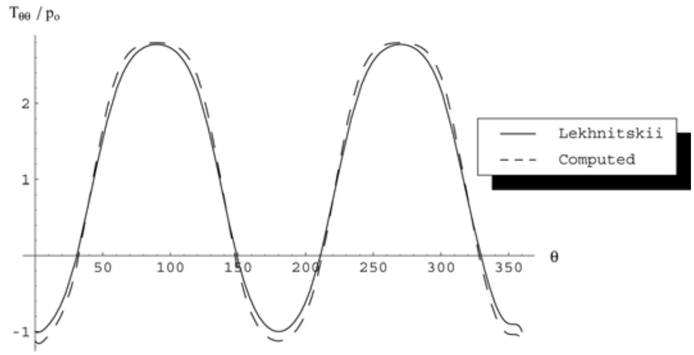

Fig. 8 Variation of dimensionless stress component, $T_{\theta\theta}/p_o$, versus θ, on the circular cavity for material III and problem 1(a), $l = 100$ cm, $r = 0.5$ cm

unknowns is 80. The variation of the stress component $T_{\theta\theta}$ versus polar angle θ has been calculated on the circular cavity for three materials for the case of problem 1(a). The results are given, for the values $l = 100$ cm, $r = 0.5$ cm in Figs. 6, 7 and 8 where θ is given in degrees. For comparison, results given by Lekhnitskii for an infinite plate for the same materials have been also presented in these Figs. $T_{\theta\theta}/p_o$ has also been calculated at A and B points for $l = 100$ cm and different r values for the same problem (Table 2), (Kadioglu and Ataoglu 2001). $T_{\theta\theta}(B)$ gives the stress concentration factor for problem 1(a).

For a finite plate, $T_{\theta\theta}(B)$ must be greater than the value given by Lekhnitskii for an infinite plate. Lekhnitskii's theoretical results for $T_{\theta\theta}(A)$ and $T_{\theta\theta}(B)$ are given in Table 3, for materials I, II and III for comparison.

The computed results given in Table 2 have been found to be greater than these values even for the smallest r which is 0.5 cm. It is seen that the presented results are compatible with those of Lekhnitskii. Stress concentration factors for the same problem have been calculated by (Vable and Sikarskie 1988) for two orthotropic materials using the same dimensions, but the uniform tension was applied in the x_2 direction (Fig. 4(b)). In the study of Vable and Sikarskie (1988), C_{lj} notation is used instead of β_{lj}, but C_{33} is taken to be equal to $0.5\beta_{66}$. Here, the same problem has been solved for the same materials to compare the results. The material constants used by Vable and Sikarskie (1988) are given in Table 4.

Table 2 Variations of dimensionless stress component, $T_{\theta\theta}/p_o$, on A and B points with the radius of the circular cavity for problem 1(a)

	Material I		Material II		Material III	
r (cm)	$T_{\theta\theta}(A)/p_o$	$T_{\theta\theta}(B)/p_o$	$T_{\theta\theta}(A)/p_o$	$T_{\theta\theta}(B)/p_o$	$T_{\theta\theta}(A)/p_o$	$T_{\theta\theta}(B)/p_o$
0.5	−0.7293	5.7408	−1.4404	4.3690	−1.1236	2.7969
1	−0.7317	5.7500	−1.4453	4.3733	−1.1254	2.7993
2	−0.7415	5.7868	−1.4650	4.3903	−1.1329	2.8086
3	−0.7579	5.8472	−1.4979	4.4185	−1.1454	2.8242
4	−0.7810	5.9299	−1.5592	4.4276	−1.1631	2.8462
5	−0.8111	6.0335	−1.6164	4.4304	−1.1860	2.8747
6	−0.8416	6.1166	−1.6843	4.4881	−1.2144	2.9100
7	−0.8850	6.2525	−1.7688	4.5553	−1.2286	2.9254
8	−0.9360	6.4033	−1.8641	4.6316	−1.2377	2.9728
9	−1.0623	6.5671	−1.9723	4.7168	−1.2496	3.0257
10	−1.2239	6.7426	−2.0937	4.8107	−1.2973	3.0861
11	−1.1384	6.9285	−2.2286	4.9130	−1.3513	3.1542
12	−1.2239	7.1240	−2.3773	5.0239	−1.4120	3.2306
13	−1.3193	7.3285	−2.5406	5.1436	−1.4799	3.3158
14	−1.4551	7.5420	−2.7190	5.2723	−1.5555	3.4105
15	−1.5421	7.7647	−2.9137	5.4106	−1.6394	3.5154

Table 3 Theoretical values of dimensionless stress component, $T_{\theta\theta}/p_o$, on A and B points given by Lekhnitskii for an infinite plate for problem 1(a)

Material I		Material II		Material III	
$T_{\theta\theta}(A)/p_o$	$T_{\theta\theta}(B)/p_o$	$T_{\theta\theta}(A)/p_o$	$T_{\theta\theta}(B)/p_o$	$T_{\theta\theta}(A)/p_o$	$T_{\theta\theta}(B)/p_o$
−0.7071	5.4530	−1.4142	4.1485	−1	2.7748

Table 4 Material constants used by Vable and Sikarskie

	β_{11}	β_{22}	β_{12}	β_{66}
Material IV	1	1	−0.25	3.3
Material V	1.96	1	−0.25	2.5

Table 5 Stress concentration factors for problem 1(b)

	Lekhnitskii	Vable and Sikarskie	Present
Material IV	3.1908	3.053	3.3251
Material V	2.5649	2.604	2.6024

Stress concentration factors, corresponding to $T_{\theta\theta}(A)/p_o$ for problem 1(b), have been calculated for materials IV and V. Results, calculated by Vable and Sikarskie (1988) and Lekhnitskii as well as those computed in this study, are given in Table 5.

It is seen from Table 5 that the present result is better than given by Vable and Sikarskie (1988) for material IV. Their result (3.053) is less than Lekhnitskii's result (3.1908), for an infinite plate.

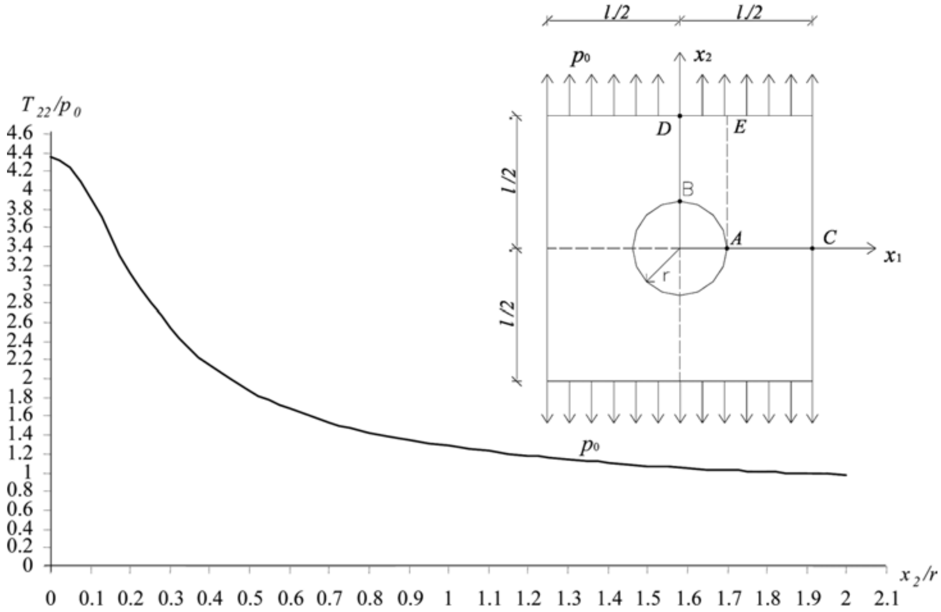

Fig. 9 Variation of dimensionless stress component, T_{22}/p_o, along line *AE* for material I

Raju *et al.* (1996) solved the same problem given in Fig. 4(b) for material I. The direction of the tension is the same as that applied by Vable and Sikarskie (1988), but it was considered that $r = a$ and $l = 20a$. The r/l ratio is greater than in the previous examples presented in this study, but the value of $T_{\theta\theta}(A)/p_o$ has been found to be quite smaller than the theoretical result given by Lekhnitskii as 4.1485, for an infinite plate. This cannot be an acceptable result. In the study of Raju *et al.* (1996), variations of the stress component T_{22}/p_o have been given along the vertical line of $x_1 = 1.0015r$ which is nearly tangent to the circular cavity at the point *A*, (Fig. 4(b), *AE* line). Here, for comparison, the same variation was calculated on $x_1 = r$ line using the same r/l ratio since we do not have any problem for calculating any stress component at the boundary and the results have been given in Fig. 9 and Table 6, for $r = 5$ cm. For an infinite plate stress concentration factor is 4.1485. Our result for $l/r = 20$ is 4.363281. Using three different method, Raju *et al.* (1996) have given the values of 3.316, 3.344 and 3.366. It seems that all of them quite smaller than the lower limit even though a big r/l ratio exists. It was thought that the difference could occur because of the small distance between the vertical lines $x_1 = r$ and $x_1 = 1.0015r$. To check this, T_{22}/p_o was calculated using present formulation at $x_1 = 1.0015r$, $x_2 = 0$ point but the result has been found as 4.294 being quite different from theirs. We presented the tables to show the differences better. Problem 1(a) was also solved by (Heng 1988), but there is no information about the material used and he has not calculated the stress concentration factor for small ratios of r/l which is significant for the accuracy of any method used.

The second sample problem is a square orthotropic plate but having an elliptical hole stretched by forces parallel to x_2 axis (Fig. 10).

The equation of an elliptical contour in the parametric form is

$$x = a\cos\vartheta, \qquad y = b\sin\vartheta \tag{28}$$

where a and b are the lengths of the principal semi-axes of the ellipse, and ϑ is the parameter

Table 6 Variation of dimensionless stress component, T_{22}/p_o, along AE line for material I and problem 1(b)

x_2/r	T_{22}/p_o
0	4.363281
0.05	4.2406019
0.1	3.9141748
0.15	3.5095652
0.2	3.1285144
0.25	2.8053583
0.3	2.5404175
0.35	2.3240318
0.4	2.1461556
0.45	1.9985067
0.5	1.8746809
0.55	1.7698358
0.6	1.6803268
0.65	1.6034028
0.7	1.5369765
0.75	1.4794509
0.8	1.4295703
0.9	1.3484653
1	1.2845892
1.1	1.2296805
1.2	1.181218
1.3	1.1393909
1.4	1.1038102
1.5	1.0736358

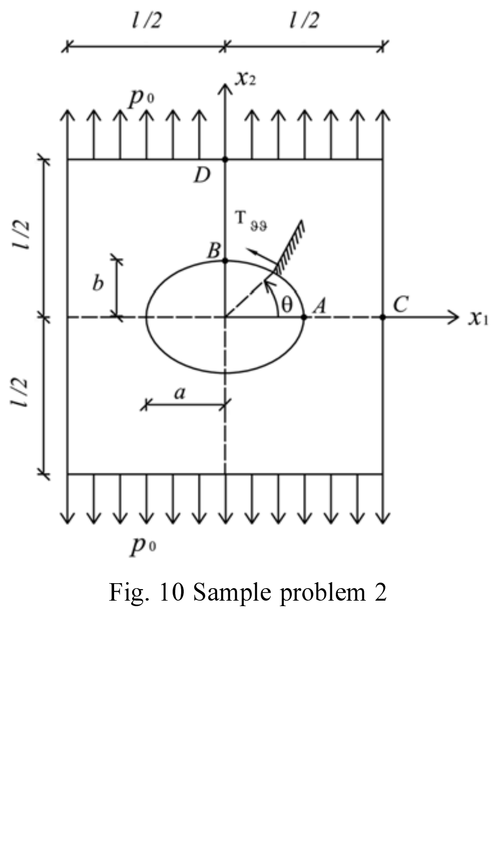

Fig. 10 Sample problem 2

which assumes all values from zero to 2π for a complete circuit of the contour. The theoretical solution of this problem for an infinite plate was also solved by Lekhnitskii (1947, 1963, 1968). If the semi-axes a and b of the ellipse are relatively small in comparison to l, the value of stress component $T_{\vartheta\vartheta}/p_o$ at point A must approach from above to the theoretical result given by Lekhnitskii for an infinite plate. To verify this, $T_{\vartheta\vartheta}(A)/p_o$ and $T_{\vartheta\vartheta}(B)/p_o$ values were calculated for different ratios of a/b for material I and $l = 100$ cm, $b = 0.5$ cm (Table 7). It is interesting that $T_{\vartheta\vartheta}(B)/p_o$ remains nearly constant for different a values. Lekhnitskii's result for $T_{\vartheta\vartheta}(B)/p_o$ has also been found out to be independent from a/b ratio for an infinite plate and for material I being equal 1.4142. The variation of $T_{\vartheta\vartheta}(B)/p_o$ was also calculated on the boundary of the elliptical cavity by choosing $l = 100$ cm, $a = 0.7$ cm and $b = 0.5$ cm (Fig. 11). It must be emphasized that θ indicates the polar angle.

Table 7 Variations of dimensionless stress components, $T_{\vartheta\vartheta}(A)/p_o$ and $T_{\vartheta\vartheta}(B)/p_o$, with the ratio of a/b for the elliptical cavity, $b = 0.5$ cm and $l = 100$ cm and material I

	Present solution		Lekhnitskii
a/b	$T_{\vartheta\vartheta}(A)/p_o$	$T_{\vartheta\vartheta}(B)/p_o$	$T_{\vartheta\vartheta}(A)/p_o$
1.2	5.0413	−1.4541	4.78
1.4	5.6954	−1.4591	5.4104
1.6	6.3283	−1.4596	6.040
1.8	6.9381	−1.4579	6.6706
2	7.5239	−1.455	7.307
2.2	8.085	−1.4515	7.9307
2.4	8.622	−1.4476	8.5608
2.6	9.7087	−1.4376	9.1909
2.8	10.3601	−1.4357	9.821
3	11.0025	−1.434	10.451
3.2	11.6351	−1.4324	11.0811
3.4	12.2575	−1.431	11.7111
3.6	12.8693	−1.4296	12.3412
3.8	13.4704	−1.4284	12.9713
4	14.0605	−1.4273	13.6013

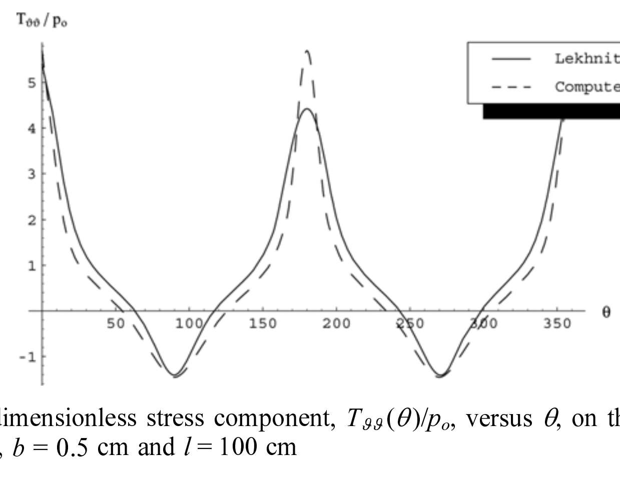

Fig. 11 Variation of dimensionless stress component, $T_{\vartheta\vartheta}(\theta)/p_o$, versus θ, on the elliptical cavity for material I, a = 0.7 cm, b = 0.5 cm and l = 100 cm

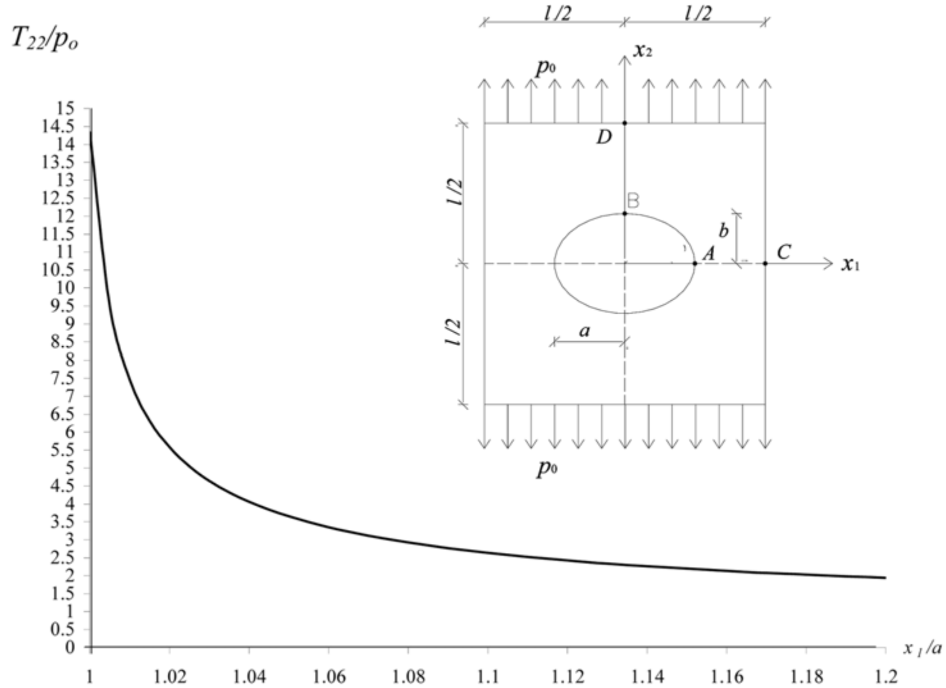

Fig. 12 Variation of dimensionless stress component, T_{22}/p_o, along the horizontal symmetry axis for sample problem 2, material I, a = 5 cm and l = 100 cm

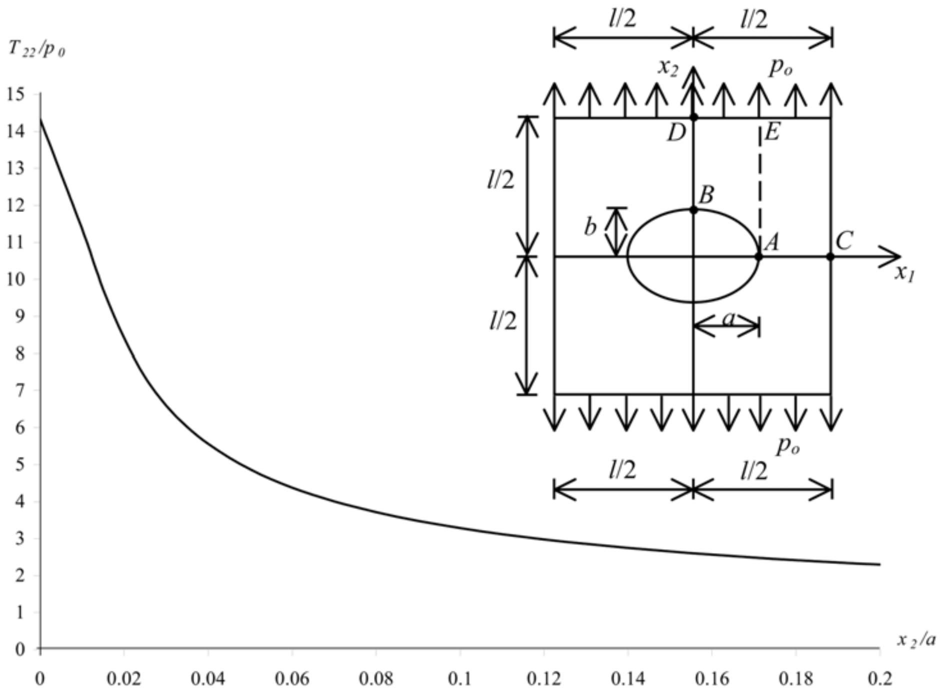

Fig. 13 Variation of dimensionless stress component, T_{22}/p_o, along the line AE for material I

Table 8 Variation of dimensionless stress component, T_{22}/p_o, along the horizontal symmetry axis for problem 2 and material I

x_1/a	T_{22}/p_o
1	14.33708
1.005	9.507749
1.01	7.456024
1.015	6.321028
1.02	5.578929
1.025	5.046719
1.03	4.641871
1.035	4.321044
1.04	4.059035
1.045	3.840065
1.05	3.653693
1.055	3.492701
1.06	3.351916
1.065	3.227528
1.07	3.116655
1.075	3.017076
1.08	2.927048
1.085	2.845178
1.09	2.770342
1.095	2.70162
1.1	2.638251
1.105	2.579599
1.11	2.525129
1.115	2.474385
1.12	2.426979
1.125	2.382575
1.13	2.340885
1.135	2.301654
1.14	2.264662
1.145	2.229714
1.15	2.196637
1.155	2.165281
1.16	2.135507
1.165	2.107196
1.17	2.080237
1.175	2.054533
1.18	2.029994
1.185	2.006542
1.19	1.984102
1.195	1.96261
1.2	1.942003

Table 9 Variation of dimensionless stress component, T_{22}/p_o, along AE line for problem 2 and material I

x_2/a	T_{22}/p_o			
	Present	Raju *et al.* 1 (Averaging approach)	Raju *et al.* 2 (Non-Averaging approach)	Raju *et al.* 3 (Discontinuous element approach)
0	14.33708			
0.001	13.21895	8.696	8.692	8.697
0.01	11.37188	8.134	8.134	8.137
0.02	8.422955	6.934	6.935	6.934
0.03	6.603969	5.775	5.776	5.780
0.04	5.566324	4.891	4.891	4.896
0.05	4.876935	4.257	4.258	4.262
0.06	4.383839	3.797	3.798	3.803
0.07	4.011685	3.454	3.455	3.460
0.08	3.719406	3.189	3.190	3.195
0.09	3.482877	2.978	2.979	2.985
0.1	3.286951	2.806	2.807	2.813
0.11	3.121589			
0.12	2.979847			
0.13	2.856755			
0.14	2.748655			
0.15	2.652792			
0.16	2.567049			
0.17	2.489771			
0.18	2.419648			
0.19	2.355631			
0.20	2.296869			

The same problem has been solved by Raju *et al.* (1996) with a/b = 4 and $l = 20a$ and for the same material. They have given the variation of the stress component T_{22}/p_o along both a vertical and an horizontal lines. In their study, the starting points of these two lines are very close to each other but not T_{22}/p_o values on them. It should be noted that the material constants have been given in psi in their study. In order to compare the presented results with those obtained (Raju *et al.* 1996), the variations of dimensionless stress component T_{22}/p_o were calculated along these specific lines by choosing $a = 5$ cm with the same a/b and a/l ratios for material I and shown in Figs. 12 and 13 and Tables 8 and 9. It must be indicated that Raju *et al.* (1996) had used three different methods for calculating the values of Table 9. They had been named as Averaging approach, Non-Averaging approach and Discontinuous element approach, respectively.

5. Examples for the accuracy of the presented method and comparison with FEM

To check the accuracy of the presented method one more time, two sample problems are also solved. First problem is an infinite plate with a circular hole under tension p_o in the x_1 direction

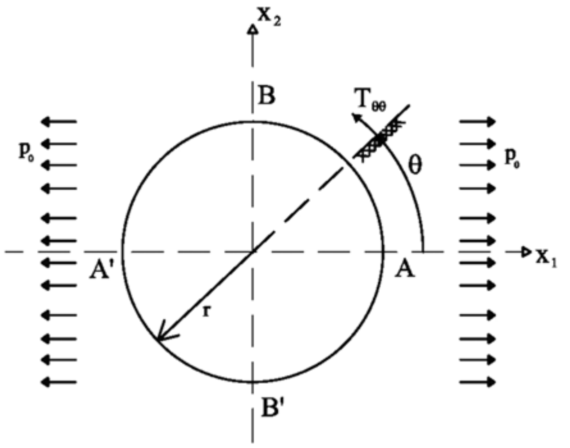

Fig. 14 Sample problem 1(c)

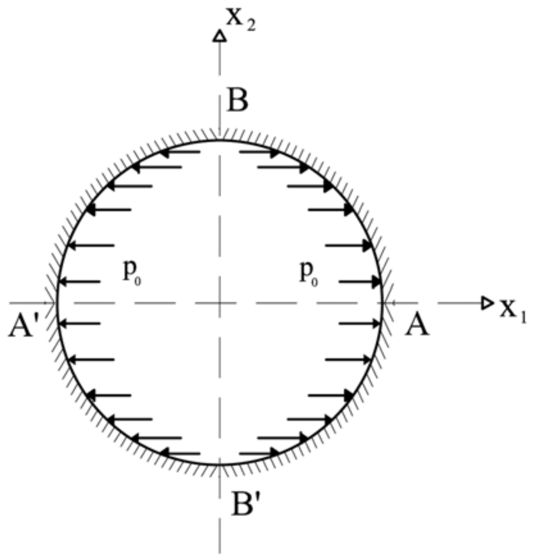

Fig. 15 First stage of problem 1(c)

(Problem 1(c)), (Fig. 14). To handle this problem, the loading in Fig. 15 is considered as the first step. In that stage, on the circular hole in the infinite plate, an uniform surface traction p_o in the x_1 direction on the segment BAB' and on the segment $BA'B$ the same p_o in the opposite direction are considered. The boundary values of the displacement, strain and stress components $(T'_{11}, T'_{12}, T'_{22})$ related to this problem can be calculated following the same procedure explained in Sect. 3. The actual stress field (T_{11}, T_{12}, T_{22}), corresponding to the loading in Fig. 14 (problem 1(c)) can be calculated as follows:

$$T_{11} = T'_{11} + p_o$$

$$T_{12} = T'_{12}, \qquad T_{22} = T'_{22}$$

After calculating the stress values on the boundary the unknown stress component $T_{\theta\theta}$ can be calculated for different values of θ in the interval of [0, 2π] for problem 1(c). Variation of $T_{\theta\theta}/p_o$ versus θ are given in Fig. 16 for material I with the theoretical results of Lekhnitskii for the same material. But during the determination of stress components on the boundary the stress components cannot be calculated on B and B' points for that problem. These points become artificial nodal points because of the discontinuity of the surface traction. But, the stresses can be calculated on the other points and values of $T_{\theta\theta}$ are compatible with those given by Lekhnitskii. This kind of approximation gives good results for a crack problem in an infinite plate because the end points of crack have already stress singularities. Of course, during calculation of the coefficient of the matrices **A** and **K** some singularities arise on the boundary elements including B and B' points. Let the numbers of the elements including B and B' points be M and $N-M$, respectively. The construction of the matrix **A** given by Eq. (21) does not produce any additional singularity problem. But, during construction of **K** matrix some singularity problems arise. The components of **K** matrix have been defined by Eq. (22). In these expressions if I and J equal to M or $N-M$, the first

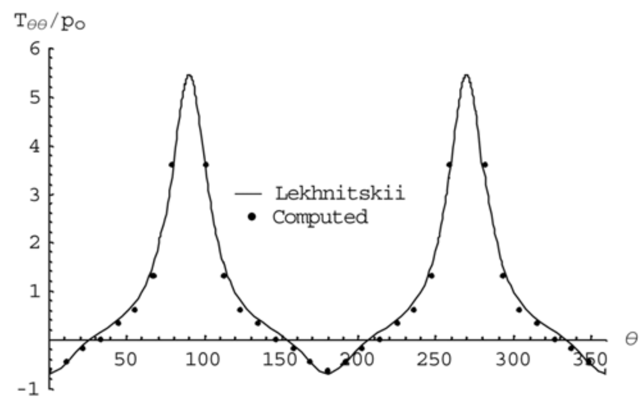

Fig. 16 Variation of $T_{\theta\theta}/p_o$ versus θ for material I (sample problem 1(c))

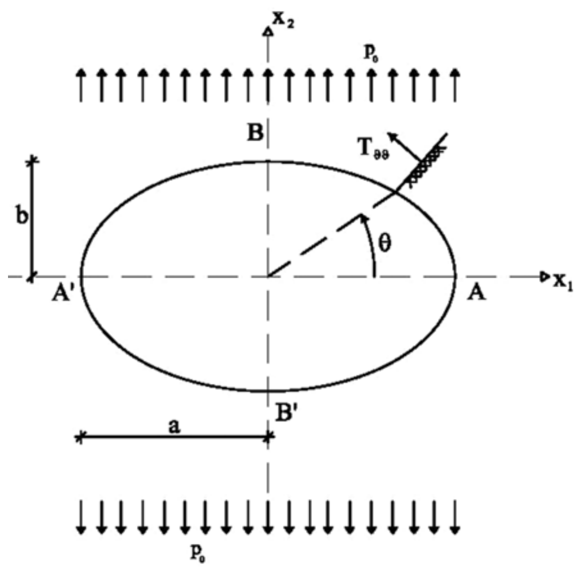

Fig. 17 Sample problem 1(d)

integrals, in the expressions of K_I and $K_{(I+N)}$ given by Eq. (22), do not produce any singularity. The second terms in these expressions are singular but they vanish since $t_2(\mathbf{x})$ is zero.

The second sample problem to check the accuracy of the presented method is an infinite plate with an elliptical hole, under tension p_o in the x_2 direction (Problem 1(d)), (Fig. 17). To solve this problem, the loading in Fig. 18 is considered as the first step. In that stage, on an elliptical hole in the infinite plate an uniform surface traction p_o in the x_2 direction on the segment $A'BA$ and on the segment $A'B'A$ the same p_o in the opposite direction are considered. The boundary values of the displacement, strain and stress components $(T'_{11}, T'_{12}, T'_{22})$ related to this problem can be calculated using the presented method, the actual stress field T_{11}, T_{12}, T_{22} corresponding to the loading in Fig. 17, can be calculated as follows:

$$T_{22} = T'_{22} + p_o$$

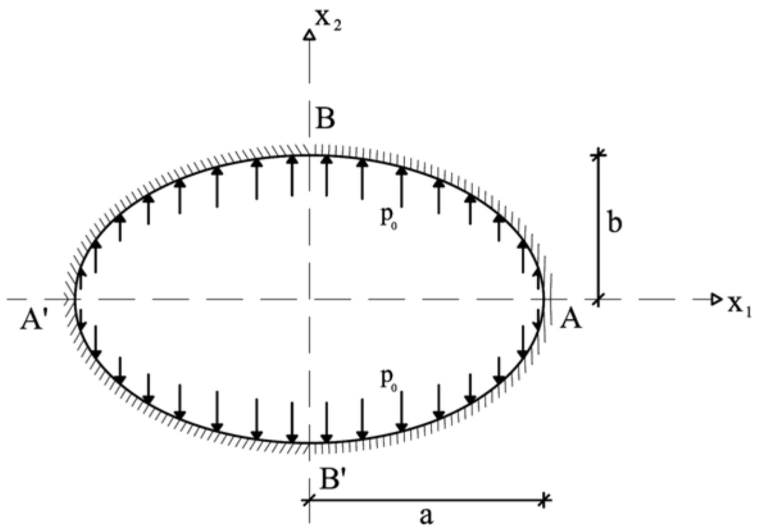

Fig. 18 First stage of problem 1(d)

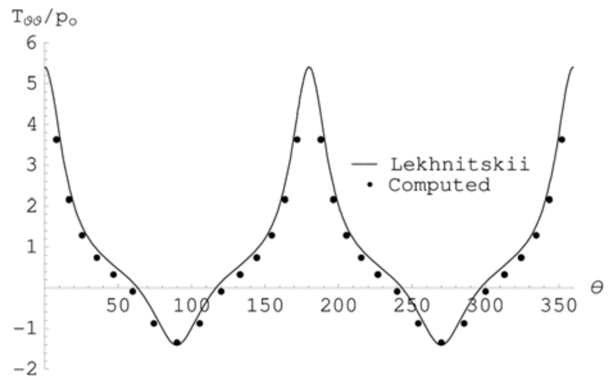

Fig. 19 Variation of $T_{\vartheta\vartheta}(\theta)/p_o$ versus θ for material I (sample problem 1(d))

$$T_{11} = T'_{11}, \qquad T_{12} = T'_{12}$$

After calculating the stress values on the boundary, the unknown stress component $T_{\vartheta\vartheta}$ can be calculated for different values of ϑ in the interval of $[0, 2\pi]$ for problem 1(d). Variation of $T_{\vartheta\vartheta}/p_o$ versus polar angle θ are given in Fig. 19 for material I with the theoretical results of Lekhnitskii for the same material. But during the determination of stress components on the boundary the stress components cannot be calculated on A and A' points. These points also become artificial nodal points because of the discontinuity of the surface traction. But, the stresses can be calculated on the other points and values of $T_{\vartheta\vartheta}$ are compatible with those given by Lekhnitskii. Let the numbers of the elements including A and A' points be M and $N - M$, respectively. The construction of the matrix **A** given by Eq. (21) does not produce any additional singularity problem. But, during construction of **K** matrix some singularity problems arise. The components of **K** matrix have been defined by Eq. (22). In these expressions if I and J equal to M or $N - M$ the second integrals, in the expressions of K_I and $K_{(I+N)}$ given by Eq. (22), do not produce any singularity. The first terms in these expressions are singular but they vanish since $t_1(\mathbf{x})$ is zero.

Moreover, to check the accuracy of the presented results for finite plate problems, two of the sample problems which have been solved by the presented method, are also solved by finite element method. The details are explained below. The problem 1(b) is solved for both materials IV and V by finite element method. The results are determined using ANSYS 10.0. The element type is PLANE82. Only a quarter of the plate is modelled since the problem is completely symmetric with respect to the horizontal and vertical centerlines. Since the purpose is to determine the stress concentration factor, a mesh is created that gets finer in the neighbourhood of the hole. To perform this, the number of divisions and spacing ratio of selected lines are defined. For grading, the left and bottom lines of the region are used. The same spacing ratio (=0.25) is used since both lines have the same length. Both lines are divided into 500. The curve that defines the hole is also divided into 40 divisions. But the spacing ratio does not specified in this case. Size level was changed 1 (fine) for the SmartSize command to generate the mesh. The next commands specify the element shape to be used for meshing and whether mapped or free meshing. Quad and free are selected in this meshing. And then, modify mesh command is selected to refine the nodes around the hole. The level of refinement was changed to 5 (maximum). The next command specify symmetry boundary conditions along the left and bottom lines. Later, the pressure is applied to the top line changing its sign from plus to minus. The 86115 nodes and 28096 elements were used for the analyses (Fig. 20). The ANSYS results are given in Table 10 for comparison with Table 5.

In the finite element analysis of elliptical hole case (Fig. 21) for material I, the same way

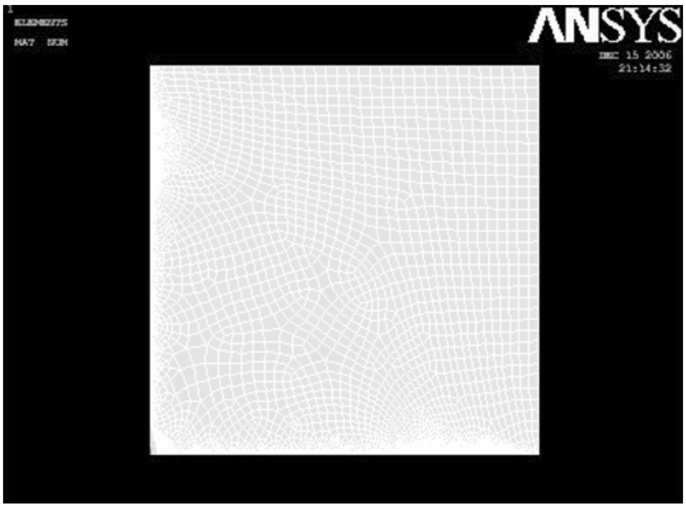

Fig. 20 Finite element mesh of problem 1(b) for materials IV and V

Table 10 Stress concentration factors for problem 1(b) with FEM, $r = 0.5$ cm and $l = 100$ cm

	FEM
Material IV	3.1993
Material V	3.0815

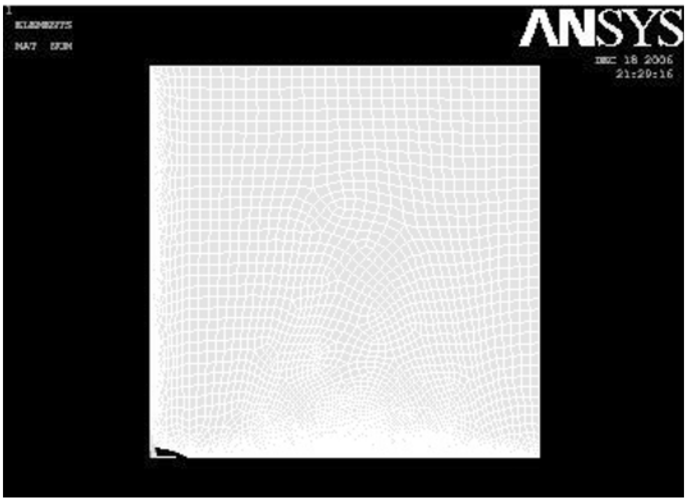

Fig. 21 Finite element mesh of problem 2 for material I

Table 11 Variation of dimensionless stress component, T_{22}/p_o, along AE line for problem 2 and material I with FEM, $a = 5$ cm, $b = 1.25$ cm and $l = 100$ cm

x_2/a	T_{22}/p_o (FEM)
0.01	9.5013
0.02	6.9591
0.03	5.6513
0.04	4.8515
0.05	4.3142
0.06	4.0322
0.07	3.7895
0.08	3.5703
0.09	3.3706
0.1	3.2238
0.11	3.0397
0.12	2.8796
0.13	2.7849
0.14	2.6933
0.15	2.6143
0.16	2.5448
0.17	2.4745
0.18	2.4
0.19	2.3388
0.20	2.2783

explained above is followed. But, the curve that defines the elliptical hole was divided into 200 divisions, so mesh has not been modified. 30339 nodes and 9706 element were used. For comparison, the results are given in Table 11 for comparison with Table 9.

6. Conclusions

A few improvements are introduced to the solutions of plane problems of linear orthotropic elasticity by reciprocal theorem. This theorem gives an integral equation for a first boundary-value problem. Unknowns of this integral equation are the boundary values of the displacement components. This integral equation can be solved using boundary elements. The aim of this study is to eliminate all of the singularities which occur during the reduction of this integral equation to a system of linear algebraic equations. To eliminate the singularities, at first, an artificial boundary for each nodal point is defined. This boundary involves boundary elements and a small arc centered at a nodal point, but, the location of this nodal point must remain outside of the artificial boundary during this process. This artificial boundary eliminates **C** matrix in classical boundary element formulation. Here, the integrals, over boundary elements and the added small arc, have been determined analytically. This small arc was shrunk to the nodal point after the calculation of the required integrals over it. It is assumed that the displacement components are constant, but no stress on this small arc. The singularities arising during calculation of the integrals over adjacent elements at the nodal point are mutually eliminated. In this study, the number of nodal points has been selected to keep the element length constant for different examples. This constant length is determined by trying a different number of boundary elements for each problem. The required element length is achieved if the results remain nearly constant for a further increment in the number of boundary elements. Kernels of the integral equation mentioned above are complex. An algorithm is introduced for the calculation of the multi-valued complex integrals over the boundary elements and the small arc mentioned above. After finding the displacement components on the boundary, the unknown stress or any displacement component can be calculated on any point inside or on the boundary without any singularity problem. But, in this case, the term corresponding **C** matrix will be taken to be equal to unity instead of zero. There is a difficulty to calculate the unknown stress component on the boundary in classical formulation, which is named as boundary layer effect (Avila *et al.* 1997). There is no boundary layer effect in this study. There are two restrictions in this method. Stresses cannot be calculated at a nodal point and also, if the surface traction vector has a discontinuity on a point of the boundary, stress components cannot be calculated on that point. If a singular load exists at any point on the boundary, this point must not be selected as a nodal point either because of second assumption on circular arc about a nodal point.

Two different problems are selected to check the accuracy of the presented formulation and for comparison with other studies. Analytical solutions of these problems have been given by Lekhnitskii for an infinite plate. Results are compatible with those of Lekhnitskii. Moreover, the present results seem better than those of the others cited. Their results were also indicated for comparison.

The case when $2\beta_{11} + \beta_{66} = 2\sqrt{\beta_{11} + \beta_{22}}$ is named as mathematically degenerate materials. Isotropic materials are a special case of those. And for this kind of materials given formulation fails. To handle this a limiting process is necessary. It was planned to consider this group of material in another work.

Moreover, to check the accuracy of the presented method, problem 1(a) and problem 2 have been solved for an infinite plate and the results have been compared with Lekhnitskii. But, in the elements on which the stress concentration factor will be calculated, a surface traction discontinuity arises just on the necessary point of these elements. Because of the first restriction of the presented method, the calculation of stress concentration factor fails. Because of this restriction the approach by increasing dimensions of the plate gives better results. Specially for stress concentration factor. However, values of the unknown stress component on the circular or elliptical boundary are the same with theoretical results for other boundary points.

Besides, for another comparison, the finite plate problem for a circular and elliptical hole are also solved by finite element method. In the presented method, number of the elements on the boundary is maximum 128. For small holes, 32 elements are used. To determine the stress distribution on a certain line or on the boundary it can be considered that additional 128 points are more than enough. But, minimum element number is 9706 in FEM.

References

Avila, R.V., Mantič, V. and París, F. (1997), "Application of the boundary element method to elastic orthotropic materials in 2D: Numerical aspects", *Proc. Boundary Elements XIX*, pp.55-64, CMP, Southampton.

Benjumea, R. and Sikarskie, D.L. (1972), "On the solution of plane, orthotropic elasticity problems by an integral method", *J. Appl. Mech.,* ASME, **39**(3), 801-808.

Berbinau, P. and Soutis, P. (2001), "A new approach for solving mixed boundary value problems along holes in orthotropic plates", *Int. J. Solids Struct.*, **38**(1), 143-159.

Deb, A. and Banerjee, P.K. (1990), "BEM for general anisotropic 2D elasticity using particular integrals", *Commun. Appl. Numer. Meth.*, **6**(2), 111-119.

Heng, Z. (1988), "Boundary element study of an anisotropic plate", *Commun. Appl. Numer. Meth.*, **4**(4), 557-559.

Jiang, L.Z. and Lee, J.S. (1994), "Plane orthotropic layer by transfer matrix-spline boundary element", *J. Appl. Mech.,* ASCE, **120**(5), 1026-1041.

Kadioglu, N. and Ataoglu, S. (1999), "An extension of boundary element method for multiply connected regions", *Boundary Elements XXI*, pp.249-258, Witpress, Southampton.

Kadioglu, N. and Ataoglu, S. (2001), "An extension of the boundary element method in orthotropic materials for multiply connected regions", *Boundary Elements XXIII*, pp.423-432, Witpress, Southampton.

Lee, J., Choi, S. and Mal, A. (2001), "Stress analysis of an unbounded elastic solid with orthotropic inclusions and voids using a new integral equation technique", *Int. J. Solids Struct.*, **38**(16), 2789-2802.

Lekhnitskii, S.G. (1947), *Anisotropic Plates*, Goverment Publishing House, M-L (Russian edition), pp.88-119, OGIZ, Gostekhizdat.

Lekhnitskii, S.G. (1963), *Theory of Elasticity of an Anisotropic Elastic Body*, Holden-Day, Inc., pp.153-174, San Francisco.

Lekhnitskii, S.G. (1968), *Anisotropic Plates*, Gordon and Breach, pp.157-217, New York.

Mantič, V. and París, F. (1995), "Explicit formulae of the integral kernels and C-matrix in the Somigliana identity for orthotropic materials", *Eng. Anal. Bound. Elem.*, **15**(3), 283-288.

Padhi, G.S., Shenoi, R.A., Moy, S.S.J. and Hawkins, G.L. (2000), "A quadratic boundary element implementation in orthotropic elasticity using the real variable approach", *Commun. Numer. Meth. En.*, **16**(4), 257-266.

Raju, I.S., Sistla R. and Krishnamurthy, T. (1996), "An efficient boundary element method for computing accurate stresses in two-dimensional anisotropic problems", *Comput. Struct.*, **59**(3), 453-462.

Rizzo, F.J. and Shippy, D.J. (1970), "A method for stress determination in plane anisotropic elastic bodies", *J. Compos. Mater.*, **4**, 36-61.

Sokolnikoff, I.S. (1956), *Mathematical Theory of Elasticity*, McGraw-Hill, pp.270, New York.

Tsutsumi, T. and Hirashima, K. (2000), "Analysis of orthotropic circular disks and rings under diametrical loadings", *Struct. Eng. Mech.*, **9**(1), 37-50.

Vable, M. and Sikarskie, D.L. (1988), "Stress analysis in plane orthotropic material by the boundary element method", *Int. J. Solids Struct.*, **24**(1), 1-18.